

Morphological Correlates of Triadic Circuitry in the Lateral Geniculate Nucleus of Cats and Rats

Y.-W. Lam, C. L. Cox, C. Varela, and S. Murray Sherman

Department of Neurobiology, State University of New York, Stony Brook, New York

Submitted 15 March 2004; accepted in final form 7 September 2004

Lam, Y.-W., C. L. Cox, C. Varela, and S. Murray Sherman. Morphological correlates of triadic circuitry in the lateral geniculate nucleus of cats and rats. *J Neurophysiol* 93: 748–757, 2005; doi: 10.1152/jn.00256.2004. We used an in vitro slice preparation of the lateral geniculate nucleus in cats and rats to study morphological correlates of triadic circuitry in relay cells. The three triadic elements involve a retinal synapse onto a GABAergic dendritic terminal of an interneuron, a synapse from the same retinal terminal onto a relay cell dendrite, and a synapse from the same interneuron terminal onto the same relay cell dendrite. We made whole cell recordings and labeled cells with biocytin. Previous methods were used to identify triadic circuitry based on evidence that the retinal terminal activates a metabotropic glutamate receptor on the interneuronal terminal. Thus application of (\pm)-1-aminocyclopentane-*trans*-1,3-dicarboxylic acid (an agonist to that receptor) increases the rate of spontaneous inhibitory postsynaptic currents (sIPSCs) recorded in the relay cell, and if some of this increase remains with further addition of TTX (a TTX-insensitive response), a triad is indicated. We quantified the extent of the TTX-insensitive response and sought morphological correlates. In both rats and cats, this response correlated (negatively) with the number of primary dendrites and (positively) with polarity of the dendritic arbor. There was no correlation with cell size. Curiously, in cats, this response correlated with the presence of appendages at primary dendritic branches, but there was no such correlation in rats. These observations in cats map onto the X/Y classification, with X cells having triads, but it is not clear from our results if a comparable classification exists for rats.

INTRODUCTION

A ubiquitous feature of thalamic circuitry is a triadic synaptic arrangement that involves many of the inputs carrying information to be relayed to cortex (reviewed in Sherman and Guillery 1996). It is called “triadic,” because three synapses are involved (see Fig. 1). The clearest and most thoroughly studied example involves retinal input to the lateral geniculate nucleus in the cat. Here, a glutamatergic retinal terminal contacts both a relay cell dendrite as well as a synaptic terminal from a GABAergic interneuron, and the dendritic terminal contacts the same relay cell dendrite. These dendritic terminals are the only ones in thalamus that are both pre- and postsynaptic. In the A layers of the cat’s lateral geniculate nucleus, many retinal terminals are involved in such triads, and this is a signature of the X cell pathway (reviewed in Sherman and Guillery 1996, 2004a,b); other retinal terminals contact relay cell dendrites in simple synapses without involvement of terminals from dendrites of interneurons, and this is typical of the Y cell pathway.

Present address and address for reprint requests and other correspondence: S. M. Sherman, Dept. of Neurobiology, Pharmacology and Physiology, The University of Chicago, 947 E. 58th St., MC 0926, 316 Abbott, Chicago, IL 60637 (E-mail: msherman@bsd.uchicago.edu).

However, the distinction is not absolute because a small minority of retinal inputs to X cells is nontriadic, ending in simple contacts onto a relay cell dendrite, and vice versa for Y cells.

In an attempt to begin to unravel the function of the triad in the cat’s lateral geniculate nucleus, we have recently confirmed previous immunocytochemical evidence (Godwin et al. 1996) that the synapse from the retinal terminal to the dendritic terminal of the interneuron activated a metabotropic glutamate receptor (mGluR) (Cox and Sherman 2000). This was accomplished by recording spontaneous GABAergic inhibitory postsynaptic currents (sIPSCs) from relay cells, and showing that, for some relay cells, an increase in sIPSCs evoked by application of a general mGluR agonist, (\pm)-1-aminocyclopentane-*trans*-1,3-dicarboxylic acid (ACPD), was only partially reduced by subsequent application of tetrodotoxin (TTX), and, for other cells, TTX completely blocked the ACPD-evoked sIPSCs. The former result, which was called “TTX-insensitive,” was interpreted to reflect the activation of mGluRs on dendritic terminals of interneurons by ACPD, indicating the presence of triadic circuitry, and the latter result, called “TTX-sensitive,” indicated that all GABAergic inputs were carried to the recorded cells by axons, suggesting little or no triadic circuitry. Furthermore, subsequent staining of these cells showed X cell morphology for the former and Y cell morphology for the latter (Cox and Sherman 2000).

However, in this prior study, the correlation between TTX sensitivity and relay cell morphology was limited to a small number of neurons that were clearly distinguishable into relay X and Y neurons based on their dendritic morphology (Friedlander et al. 1981; Stanford et al. 1983). The majority of neurons were not clearly distinguishable as X or Y based on the morphology alone and were therefore not included in that analysis. Considering the possibility of intermediate morphological or physiological responses, this leaves open the question as to whether the degree of “TTX-insensitivity” can be used as an in vitro means of classifying cat geniculate cells as X or Y. We thus aimed to quantify both functional features of TTX sensitivity and morphological parameters in cat geniculate cells to determine if these are bimodally distributed, thereby suggesting something akin to an X/Y classification.

In situ hybridization and immunocytochemistry have shown that, within the thalamus of the rat, there is expression of mGluR1 (Fotuhi et al. 1993; Shigemoto et al. 1992), mGluR4 (Tanabe et al. 1993), mGluR5 (Romano et al. 1995; Tanabe et al. 1993), and mGluR7 (Okamoto et al. 1994; Tanabe et al.

The costs of publication of this article were defrayed in part by the payment of page charges. The article must therefore be hereby marked “advertisement” in accordance with 18 U.S.C. Section 1734 solely to indicate this fact.

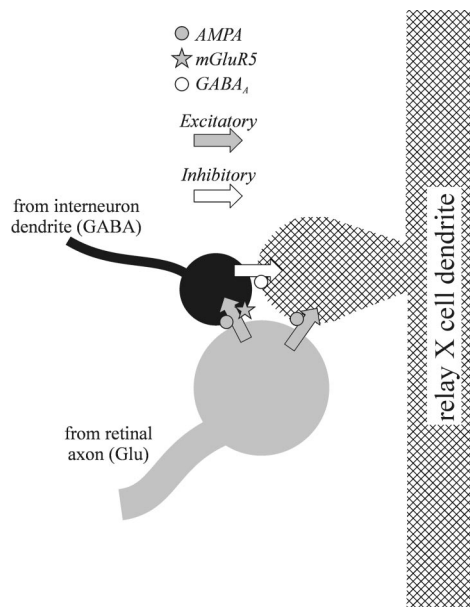


FIG. 1. The triad in the cat's lateral geniculate nucleus shown schematically. The triad consists of 3 synapses: from the retinal terminal to the relay cell and to the GABAergic, dendritic terminal of the interneuron and from this interneuron terminal to the same relay cell. The retinal terminal activates AMPA receptors on the relay cell and also *N*-methyl-D-aspartate (NMDA) receptors (not shown). The retinal terminal also activates metabotropic glutamate receptor (mGluR) and AMPA receptors on the interneuron presynaptic terminal; the presence of NMDA receptors there has not been tested. The interneuron terminal activates GABA_A receptors on the relay cell; the presence of GABA_B receptors there has not been tested.

1993). At the ultrastructural level, interneurons within the rat lateral geniculate nucleus contain presynaptic dendrites and that they participate in triadic synaptic arrangements essentially the same as found in carnivores and primates (Lieberman 1973; Ohara et al. 1983). In the cat, such triadic circuitry is associated with X and not Y cells (reviewed in Sherman 1985).

The relationship between these triadic presynaptic dendrites of interneurons and postsynaptic cells types is not clear in the rat. That is, limited data suggest that the rat lateral geniculate nucleus, like that in the cat, may also consist of subtypes of relay neurons (Lennie and Perry 1981; Martin 1986; Gabriel et al. 1996), although this is contentious (Fukuda et al. 1975), and whether these triadic arrangements are limited to a specific subgroup of relay neurons is unknown. Our earlier studies in the rat lateral geniculate nucleus clearly demonstrated a TTX-sensitive and -insensitive populations of neurons in response to the ACPD, so the data are consistent but not conclusive (Cox and Sherman 2000; Govindaiah and Cox 2004). To begin to explore the generality of these properties of triads in the mammalian thalamus, we decided to extend these observations by determining if geniculate cells in the rat that are TTX-sensitive or -insensitive also have morphological correlates, and if so, how these might relate to the X and Y morphological features described for the cat.

METHODS

Preparation of thalamic slices

Thalamic slices were obtained from kittens (postnatal age: 4–8 wk) and young Sprague-Dawley rats (postnatal age: 10–18 days). The kittens were deeply anesthetized with ketamine (25 mg/kg) and

xylazine (1 mg/kg), a craniotomy was made, and a block of tissue containing the lateral geniculate nucleus was quickly removed and placed into cold, oxygenated slicing medium (~4°C) containing (in mM) 2.5 KCl, 1.25 NaH₂PO₄, 10.0 MgCl₂, 0.5 CaCl₂, 26.0 NaHCO₃, 11.0 glucose, and 234.0 sucrose. To obtain rat tissue, the animal was deeply anesthetized with pentobarbital sodium (50 mg/kg), and the brain was quickly removed and chilled in ice-cold physiological saline (ACSF, in the following text). Tissue slices (300–400 μm) were cut in either a coronal (rat and cat) or sagittal (cat) plane using a vibrating tissue slicer, transferred to a holding chamber containing oxygenated physiological saline maintained at 30°C, and incubated for ≥2 h prior to recording. The orientation used for tissue preparation (coronal, sagittal) did not influence our results and have therefore been combined.

Recording and data analysis

Whole cell recordings were performed using a visualized slice recording apparatus as described previously (Cox and Sherman 2000). The ACSF for cat slices contained (in mM) 126 NaCl, 2.5 KCl, 1.25 Na₂PO₄, 2 MgCl₂, 2 CaCl₂, 26 NaHCO₃, and 10 glucose and for rat slices contained: 125 NaCl, 3 KCl, 1.25 NaH₂PO₄, 1 MgCl₂, 2 CaCl₂, 25 NaHCO₃, and 25 glucose. Recording pipettes were pulled from borosilicate glass capillaries and had tip resistances of 4–8 MΩ when filled with an intracellular solution containing (in mM) 117 Cs-gluconate, 13 CsCl, 2 MgCl₂, 10 HEPES, 2 Na₂-TP, 0.3 Na-GTP, and 0.4% biocytin. The pH of the intracellular solution was adjusted to 7.3 with CsOH, and the osmolality was 290 mosM. Recordings were obtained using an Axoclamp 2A amplifier in continuous single-electrode voltage-clamp mode and/or Axopatch 200B in voltage-clamp mode (both from Axon Instruments, Foster City, CA). The amplitudes of spontaneous inhibitory postsynaptic currents (sIPSCs) were maximized by holding the cells at 0 mV (Cox and Sherman 2000). The K⁺ channel blocker, Cs⁺, was included in the recording pipette to suppress direct effects of metabotropic glutamate agonists on the recorded cell because these operate by reducing *I*_{K-leak}. The access resistance of the cells was constantly monitored, and recordings were limited to neurons with a stable access of <30 MΩ. Data were acquired and digitized using the pClamp software from Axon Instrument and stored on a PC compatible computer. Correlation coefficients and linear regression were calculated using Statview (SAS Institute, Cary, NC) or Origin (Microcal, Northampton, MA).

Calculations of the power spectra (Fast Fourier Transform) of recordings were done in Clampfit (Axon Instrument). Frequencies <3 Hz were omitted from analysis because these mostly reflected slow drifts of membrane current and not sIPSCs, which were the focus of the study. Because test pulses to measure access resistance were used in studies of the cat and not the rat, this affected the overall spectra and makes detailed comparison between species difficult. Nonetheless, our objective here was to compare effects of various treatments within one of the species (and usually within a cell), so this posed no problem.

All neuroactive drugs were bath applied as previously described (Cox and Sherman 2000). Because drugs were applied in this fashion, it took some time for them to reach the recording chamber, leading to long response latencies. ACPD and SR95531 were purchased from Tocris (Ellisville, MO), and all other chemicals were purchased from Sigma (St. Louis, MO).

Histology

Biocytin (0.4%) was included in the glass pipettes during recording to label the cells. After each experiment, the slices were fixed by immersion in 0.1 M phosphate buffer containing 4% paraformaldehyde. The fixed tissue was rinsed and placed in a solution of avidin-biotin-HRP complex solution (Vectastain Elite, Vector Laboratories, Burlingame, CA) overnight. The following day, the sections were

processed with diaminobenzidine (DAB) (Sigma), dehydrated, and mounted for light microscopy. Photomicrographs were taken using a digital camera. Measurement of cross-sectional cell body area and estimated cross-sectional area of the dendritic arbor were performed with the aid of a computer-controlled microscope (NeuroLucida; MicroBrightField, Williston, VT).

RESULTS

Cat geniculate cells

ACPD-INDUCED INCREASES IN sIPSCs. We re-analyzed data from 38 neurons of the cat's lateral geniculate nucleus reported previously (Cox and Sherman 2000). ACPD, bath applied at a concentration of 125–500 μM , evoked robust increases in the frequency and amplitude of sIPSCs. An example of one such experiment is shown in Fig. 2A. Sections of the recordings at an expanded time scale are also shown to illustrate the response. Application of TTX only partially reduces the ACPD-induced increase in sIPSCs (Fig. 2C).

A major goal of this study was to quantify the ACPD-induced increase in sIPSCs. To do this, we calculated the power spectra of selected regions: a 50-s period of the baseline before ACPD application and a 50- to 120-s period during the peak of the response to ACPD application (Fig. 2, A and C, gray boxes). The power spectra in Fig. 2, B and D, show that the frequency components between 3 and 30 Hz captured most of the ACPD-induced increase of sIPSCs. The sum of the power of these frequency components was therefore used as a

measure of the ACPD-evoked response. In this example, the ACPD-evoked response was 409% over the baseline (Fig. 2B), and the presence of TTX only partially reduced this to 211% over baseline. Figure 2, E and F, shows that the ACPD-evoked increase in the presence of TTX was effectively abolished by application of bicuculline methiodide (BMI), a GABA_A antagonist.

The percentage of the power at 3–30 Hz during the ACPD-evoked response over the baseline in the presence of TTX was determined, this being the measure of TTX-insensitive response, and this was used as an index of the relative extent of triadic innervation of the recorded cell. Most (29) of these were done with an ACPD concentration of 125 μM , although 7 had a concentration of 250 μM and 2 had 500 μM . Because we saw no significantly larger response at these higher concentrations (250 and 500 μM) than that at 125 μM (Mann-Whitney, $P > 0.1$), we pooled these data. Figure 3 shows the distribution of these percentages, and this was unimodally distributed. A separate measure that was also used was the ratio of this power between the ACPD-evoked increase in sIPSCs with and without added TTX, and the overall results were the same as the first measure, so only the first measure is documented here.

Figure 4 briefly summarizes the previously reported, qualitative relationship between morphology and ACPD-evoked sIPSCs (Cox and Sherman 2000). Cells with X-like morphology, including a smaller cell body and clusters of grape-like dendritic appendages at proximal branch points (Fig. 4A) had a

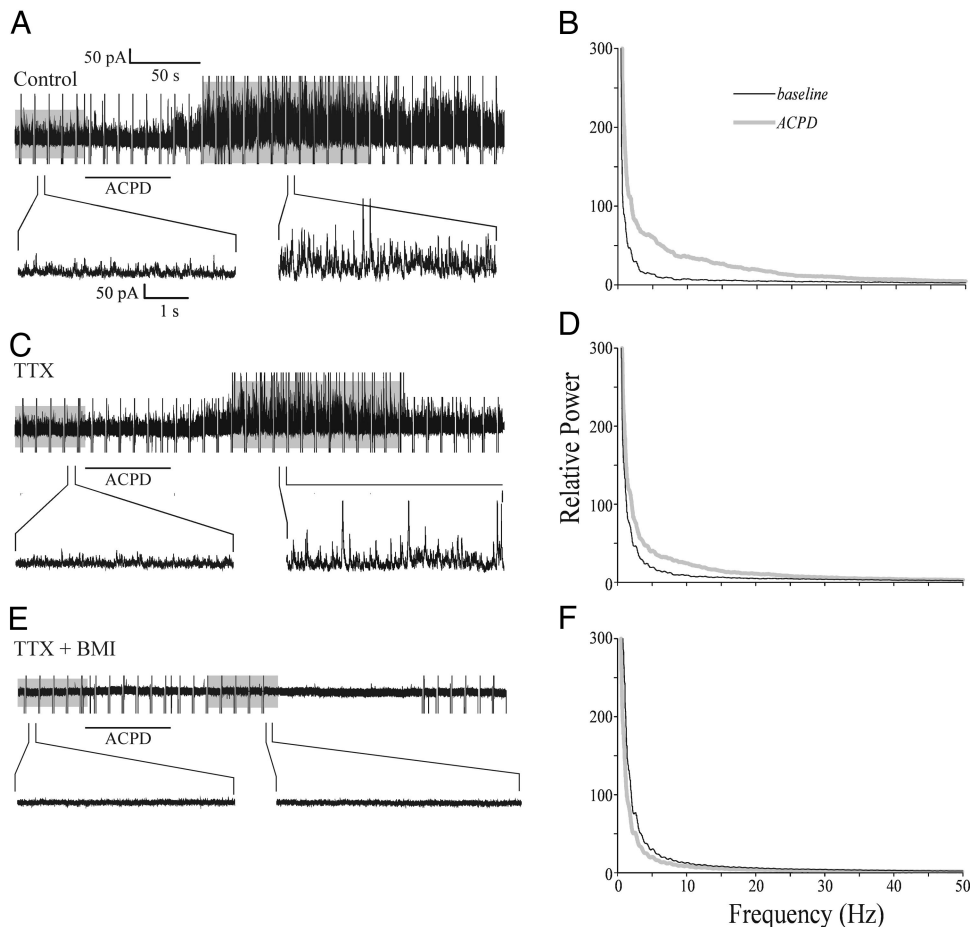


FIG. 2. Effects of (\pm)-1-aminocyclopentane-*trans*-1,3-dicarboxylic acid (ACPD) and TTX on increase of GABAergic sIPSCs recorded in voltage clamp from cat geniculate cell. *A*: application of ACPD (horizontal bar) increases the frequency and amplitude of spontaneous inhibitory postsynaptic currents (sIPSCs). To show this more clearly, expanded traces before and after ACPD application are shown below. *B*: power spectra of baseline and during ACPD-evoked response of recording shown in *A* from the regions within gray boxes. The increased amplitude and frequency of sIPSCs occurs mostly between 3 and 30 Hz. *C*: response to ACPD persists even after TTX application. Selected regions of the recording are shown in larger time scale (*bottom*). *D*: spectral analysis; conventions as in *B*. This shows the spectrum before and after ACPD application in the presence of TTX from regions within gray boxes in *C*. *E*: the TTX-insensitive response is completely abolished by the application of the GABA_A antagonist, bicuculline methiodide (BMI). Selected portions of the recording are shown in larger time scale (*bottom*). *F*: spectral analysis; conventions as in *B*. This shows the spectrum before and after ACPD application in the presence of TTX and BMI from regions within gray boxes in *E*.

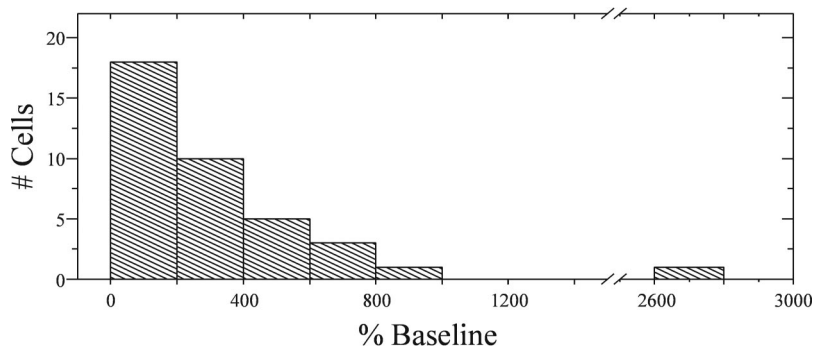


FIG. 3. Histogram showing distribution of TTX-independent effects for cat geniculate cells. The effect is calculated as percent increase of TTX-independent ACPD-evoked sIPSC activity over baseline.

distinguishable TTX-insensitive response to ACPD (Fig. 4C). A bipolar dendritic arbor is also commonly seen for X cells, but this is not evident for Fig. 4A because the plane of the slice was mostly at right angles to the long axis of the dendritic tree, which was evident from qualitative assessment of the z axis during the cell reconstruction (data not shown), but the main parameter to be shown for this analysis in any case is the presence of the dendritic appendages at branch points. In contrast, cells with Y-like morphology, including a spherical

dendritic arbor, relatively smooth dendrites, and a larger cell body (Fig. 4B) had a TTX-sensitive response (Fig. 4D).

Morphological correlates

We sought to quantify the morphology-function relationship by quantifying several morphological parameters to correlate with the measure of TTX sensitivity based on analyzing power spectra as described for Fig. 2, B, D, and F. In every case, the

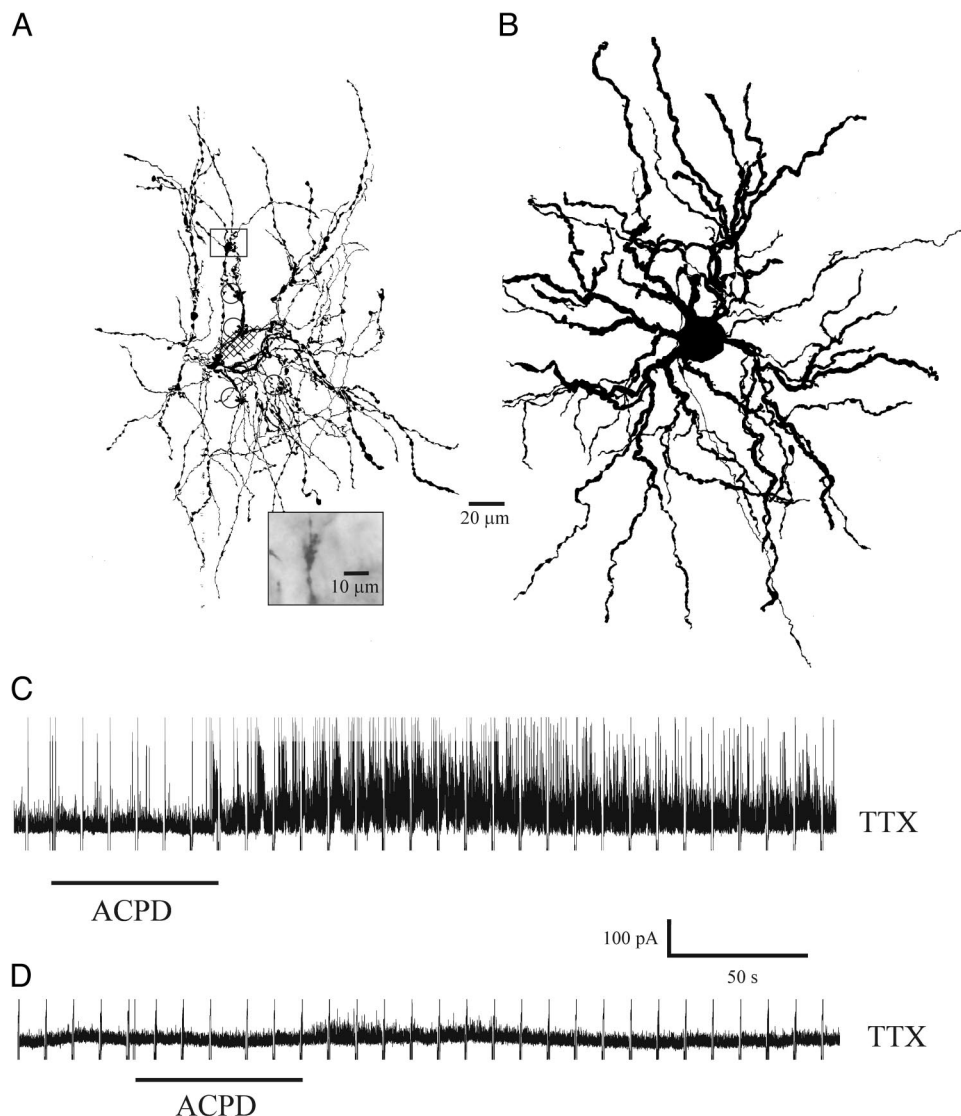


FIG. 4. Examples of cat geniculate cells showing morphology and TTX-insensitive and -sensitive response to ACPD. *A*: 2-dimensional tracing of a cell exhibiting a TTX-insensitive response to ACPD (shown in *C*). It has the typical bipolar dendritic arbor of an X cell, although it is not obvious here because the plane of the slice was mostly at right angles to the long axis of the dendritic tree. Clusters of grape-like dendritic appendages are also common near primary branch points. A photomicrograph of the cluster in the rectangle is shown at higher power (*inset*). Three other clusters are noted by circles. The cell body is cross-hatched. *B*: 2-dimensional tracing of a cell exhibiting TTX-sensitive response to ACPD (shown in *D*). It has typical Y cell morphological features, such as a radial dendritic arbor and few if any dendritic appendages. The 20- μ m scale applies to *A* and *B*. *C*: response of the cell in *A* to ACPD (125 μ M) in the presence of TTX (1 μ M). The response is only partially blocked. *D*: response of the cell in *B* to ACPD (125 μ M) is almost completely blocked by TTX (1 μ M).

individual analyzing the morphological features had no knowledge of the cell's physiological properties. This was done for a subset of 10 cells of the 38 neurons in Fig. 3, for which appropriate morphological data were available. For the remainder, cell labeling was not sufficient for proper quantification.

NUMBER OF PRIMARY DENDRITES. The number of primary dendrites were counted independently for each labeled cell by two investigators. Their numbers were averaged and rounded down. Although this morphological measure seemed to be unimodally distributed among the cells, Fig. 5A shows the significant, negative correlation between this parameter and the TTX-insensitive response ($r = -0.67$; $P < 0.05$).

DENDRITIC GEOMETRY. We used a modified Scholl ring approach to determine the geometry of the dendritic tree and thus its tendency to be bipolar versus radial. To do this, a two-dimensional reconstruction of the cell was performed, and then a circle was drawn onto the reconstruction centered on the soma; the circle was large enough to include the entire dendritic arbor. The circle was divided into quadrants by two lines passing through the center at right angles to one another. Each line was oriented 45° to the apparent long axis of the soma as judged by eye. The percentage of primary dendrites that fell within the two opposite quadrants of the circle was calculated. The same analysis was carried out twice independently and the results averaged. This parameter also was unimodally distributed, but, as indicated in Fig. 5B, it, too, showed a significant, positive correlation with the TTX-insensitive response ($r = +0.75$; $P < 0.01$).

CELL BODY SIZE. The cross-sectional area of each cell body was determined, and these values were unimodally distributed. Figure 5C shows that, in this case, there was no significant correlation between cell body size and the magnitude of the TTX-insensitive response to ACPD ($r = -0.21$, $P > 0.1$). We have also used a second approach to estimate the soma size: the cross-sectional areas of the soma at different focal planes were measured and added together to provide an estimate of volume. Soma size calculated with this method did not give significantly different results (data not shown).

NUMBER OF DENDRITIC APPENDAGES. For this analysis, we simply checked each primary dendritic branch point of every neuron for the presence of one or more appendages and expressed this for each cell as the percentage of its primary branches so endowed. This analysis was also done twice independently and the results from two investigators averaged. Of the 10 cells used in the analysis for Fig. 5, A–C, 1 had a number of artifacts near primary dendritic branch points, so this cell was not used for this final analysis. The distribution seemed to be bimodally distributed, which is also apparent in the positive correlation with TTX insensitivity shown in Fig. 5D ($r = +0.84$, $P < 0.005$). The interesting points here are that geniculate X cells in cats have many appendages at primary branch points, whereas Y cells have few, and these appendages are the postsynaptic site of triads (Friedlander et al. 1981; Hamos et al. 1987; Wilson et al. 1984).

Thus there was considerable correlation between the measure of TTX insensitivity and several morphological param-

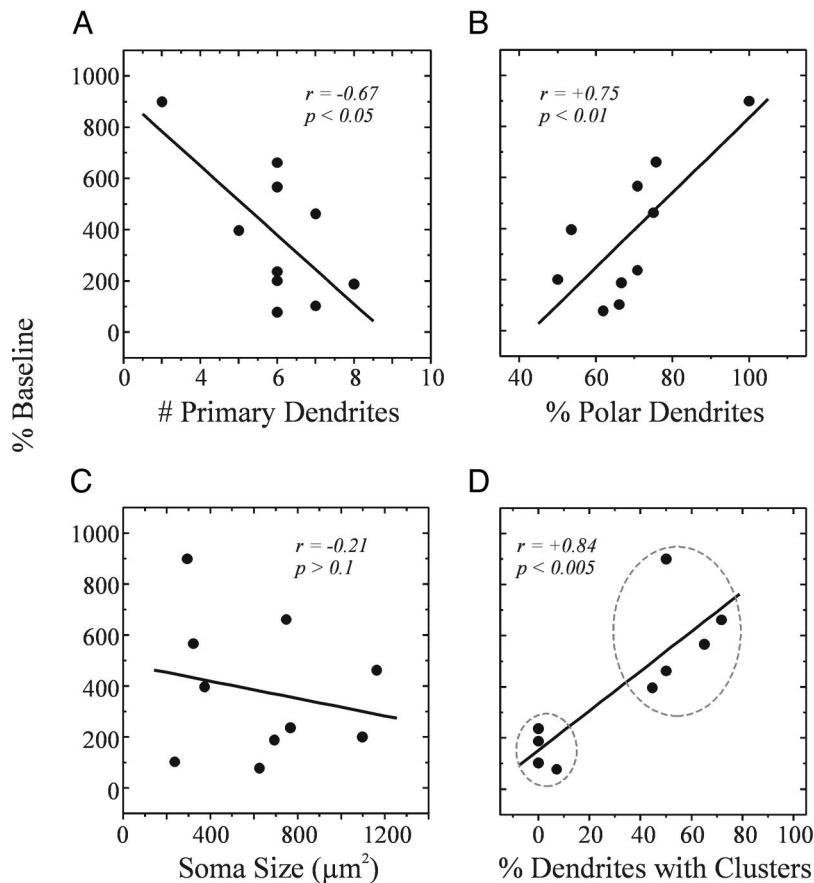


FIG. 5. Scatter plots showing measurements of morphological features of cat geniculate neurons and their relationships to the size of TTX-independent ACPD-evoked response measured as the percentage of the power between 3 and 30 Hz over the baseline. A regression line and the results of correlation analyses are shown. The number of cells is 10 for A–C and 9 for D. A: number of primary dendrites. This is significantly correlated with the magnitude of the TTX-independent response. B: percentage of polar primary dendrites. This is also significantly correlated with the size of the TTX-independent response. C: cross-sectional area of the soma. This is not significantly correlated with the size of the TTX-independent response. D: percentage of primary branch points with grape-like appendages. Not only is this significantly correlated with the size of the TTX-independent response, the relationship suggests 2 clusters (enclosed by ---).

ters, but only that involving dendritic appendages suggested clustering into two groups, presumably corresponding to X and Y.

Rat geniculate cells

ACPD-INDUCED INCREASES IN sIPSCs. As in the cat, a TTX-insensitive response, namely, an increase in IPSC activity in relay neurons after application of ACPD that persisted in the presence of TTX, indicated the presence of innervation via dendritic outputs (F2 terminals) of interneurons. Also TTX-sensitive responses were seen in which application of TTX effectively abolished the ACPD evoked increase in sIPSCs. Figures 6 and 7 demonstrate this. Figure 6 shows an example from a rat geniculate relay cell for which the ACPD-evoked increase in sIPSCs (Fig. 6A) is attenuated by SR95531, a GABA_A antagonist (Fig. 6C), and the power spectra of responses can be used to quantify these measures (Fig. 6, B and D). Figure 7 illustrates the response of rat geniculate cells to ACPD. Figure 7A shows a histogram of the distribution of the TTX-insensitive component. In 16 of the 49 cells, ACPD-evoked increases of sIPSCs were totally blocked or nearly so (<200% of baseline) by application of TTX, (example in Fig. 7B, 1 and 2), whereas 9 of the cells had a clear TTX-insensitive component (>1,000% of baseline; example in Fig. 7D, 1 and 2). The other 24 cells had intermediate responses to ACPD in the presence of TTX (example in Fig. 7C, 1 and 2).

The locations of the cells with very clear or negligible TTX-insensitive responses were plotted (data not shown). These were randomly distributed throughout the lateral geniculate nucleus. We did not see any relationship between their locations and the strength or nature of their TTX-insensitive response.

Morphological correlates

The morphology of the recovered cells varied considerably, but as in the cat, there were correlations between various morphological parameters and TTX insensitivity to ACPD-evoked sIPSCs. Figure 8 shows examples of one cell with a strong TTX-insensitive response to ACPD (Fig. 8, A and B)

and another cell with a TTX-sensitive response (Fig. 8, C and D). Figure 9 shows additional examples of relay cells included in our analysis. Figure 9, A and B, are cells with large TTX-insensitive responses and C and D are cells having small or no TTX-insensitive responses (not shown). Of interest is the observation that two of the cells (Fig. 9, A and C) have no appendages near dendritic branch points, whereas the other two (Fig. 9, B and D) have such appendages. This exemplifies a lack of correlation between this morphological feature and TTX insensitivity in the rat, despite the observation that this morphological feature correlated with TTX insensitivity quite well in the cat. As in the cat, we quantified this and other morphological features to try to establish further classification criteria with the individual analyzing the morphological features having no knowledge of the cell's physiological properties.

NUMBER OF PRIMARY DENDRITES. Figure 10A shows that although the distribution of the number of primary dendrites is unimodal, this parameter correlated negatively with the extent of TTX insensitivity of the sIPSC response to ACPD ($r = -0.43$, $P < 0.05$). This relationship is thus similar to that for the cat (see Fig. 5A).

DENDRITIC GEOMETRY. Figure 10B shows a unimodal distribution for the polarity of dendritic arbors. Nonetheless, the percentage of polar dendrites was positively correlated with the magnitude of its TTX-insensitive response to ACPD ($r = +0.52$, $P < 0.005$). Again, this relationship is similar to that for the cat (see Fig. 5B).

CELL BODY SIZE. Figure 10C shows that the resultant distribution of cell sizes is unimodal and that there was no significant correlation between cell body size and the magnitude of the TTX-insensitive response to ACPD ($r = +0.04$, $P > 0.1$).

NUMBER OF DENDRITIC APPENDAGES. Figure 10D shows that the distribution of the percentage of dendritic branch points with clusters of appendages is quite flat across the cell population. Of particular interest is the observation that this morphological parameter failed to correlate with the magnitude of its TTX-

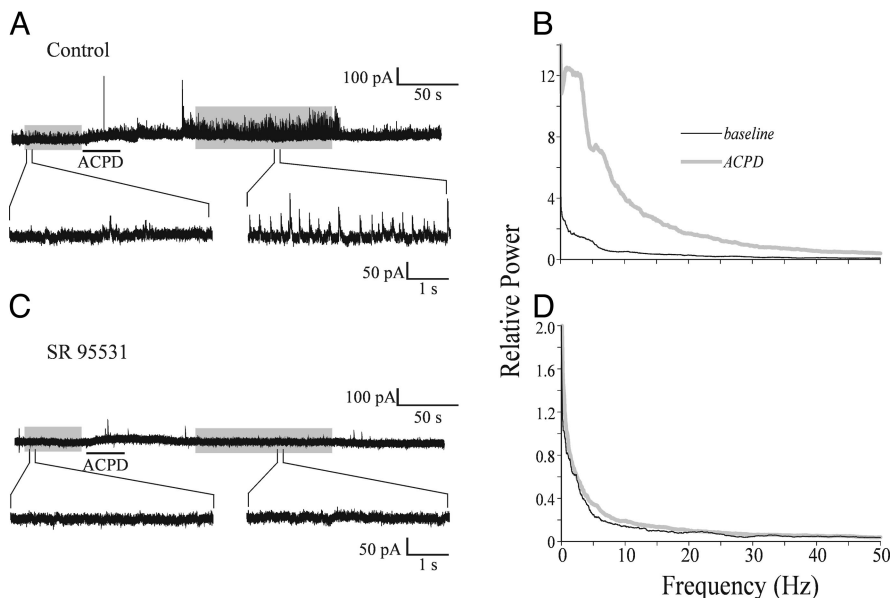


FIG. 6. ACPD-evoked increase of sIPSCs in rat geniculate neurons. All conventions for recording and power spectra as in Fig. 2. A: application of ACPD increases the frequency and amplitudes of sIPSCs; selected regions of the recording are shown in larger time scale (bottom). B: spectral analysis of regions indicated in A. C: bath application of 20 μ M SR 95531, a GABA_A antagonist, blocks the ACPD-evoked response. D: spectral analysis of regions indicated in C.

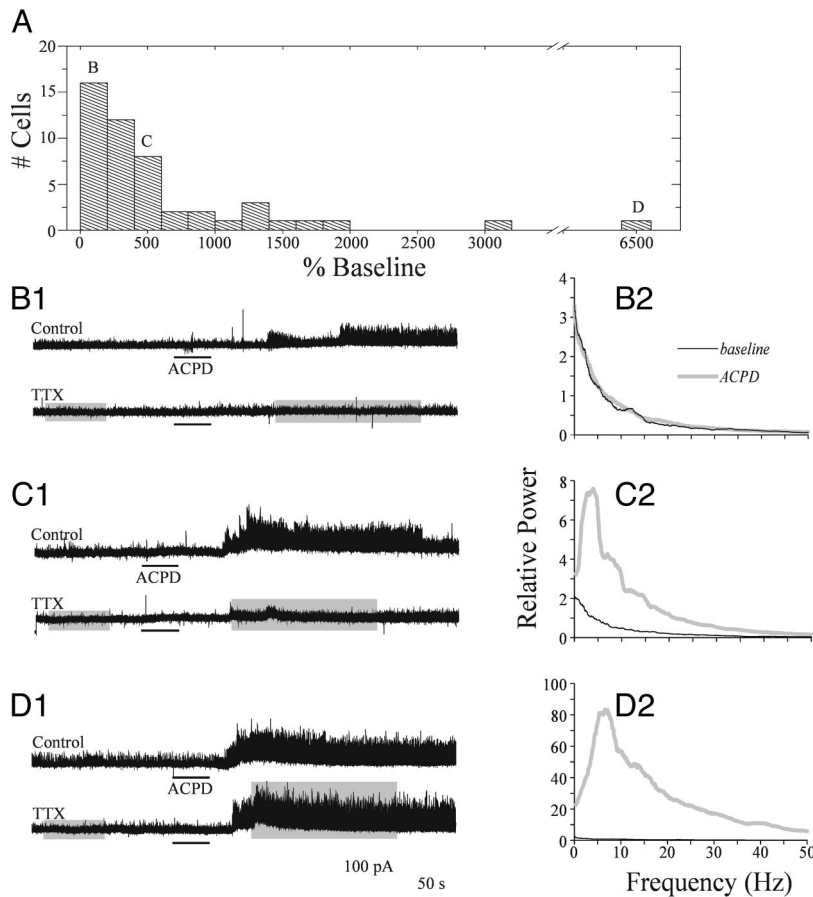


FIG. 7. TTX-sensitive and -insensitive response of rat geniculate cells with spectral analysis; conventions as in Figs. 2 and 3. *A*: histogram showing distribution of TTX-independent effect of the magnitudes of ACPD-evoked response. The letters (B–D) indicate bins from which lower examples are selected. *B1*: example of a recording in which TTX completely blocked the ACPD-evoked response. *Top*: the control; *bottom*: the recording in the presence of TTX. *B2*: spectral analysis of *B1*. *C1*: example in which a moderate response to ACPD remained in the presence of TTX. *Top*: the control; *bottom*: the recording after bath application of 1 μ M TTX. *C2*: spectral analysis of *C1*. *D1*: example in which TTX had little effect on the ACPD-evoked response. *D2*: spectral analysis of *D1*. Note the different scale of the ordinate.

insensitive response to ACPD ($r = +0.10$, $P > 0.1$). Note that this is quite different from the relationship in the cat (see Fig. 5*D*), the only correlation that did differ.

DISCUSSION

Our data indicate that the relative contribution to relay cells of the lateral geniculate nucleus in cats and rats of inhibitory synapses from presynaptic dendrites of interneurons, as measured pharmacologically *in vitro*, correlates with a number of morphological parameters. Specifically, the larger this relative contribution, the more bipolar the dendritic arbor and the fewer the primary dendrites. In the cat, this contribution also correlates with the presence of dendritic appendages at primary branches, but, interestingly, there is no such correlation for the rat. For the cat's lateral geniculate nucleus, these morphological features characterize relay X cells (Friedlander et al. 1981; Stanford et al. 1983), and the relationship involving dendritic appendages suggests clustering into discrete X or Y classes (Fig. 5*D*). Although the rat geniculate cells show many similarities in this analysis to those of the cat, the difference involving appendages and failure to show any clustering fail to provide support for a similar classification.

Observations in the cat

However, it is interesting to compare the morphological correlates determined here *in vitro* with those determined *in vivo* for X and Y cells in the cat (Friedlander et al. 1981; Stanford et al. 1983). It was shown that Y cell bodies were, on average larger than those of X cells, but that the overall size distribution was unimodal, and so it is perhaps not surprising that we failed to find a correlation of cell body size with the extent of TTX independence of ACPD-evoked sIPSCs (Fig. 5*C*). Although Friedlander et al. (1981) used a different analysis to estimate polarity of the dendritic arbor, their Fig. 25 indicates a correlation with cell type that nonetheless shows a unimodal distribution, much like the analysis of Fig. 5*B*. Furthermore, while these authors did not quantify the distribution of appendages, they noted that these were characteristic of X but not Y cells, in agreement with Fig. 5*D*. Friedlander et al. (1981) did not quantify number of primary dendrites, so there is no *in vivo* data available to compare with Fig. 5*A*.

Mainly the observations reported here extend those made previously (Cox and Sherman 2000) by quantifying the relationship between physiological and morphological variables and also clarifying the use of these criteria to permit identification of X and Y cells *in vitro*. In particular, Fig. 5*D* shows that the parameter of clusters of dendritic appendages (the abscissa in the graph) is bimodally distributed and thus can be used alone to identify X versus Y. However, Fig. 5*D* also shows that TTX sensitivity (the ordinate in the graph), although correlated with the X/Y classification, is continuously distributed, and so unless the measure of sensitivity is at one of the extremes, this cannot be used confidently to identify cell

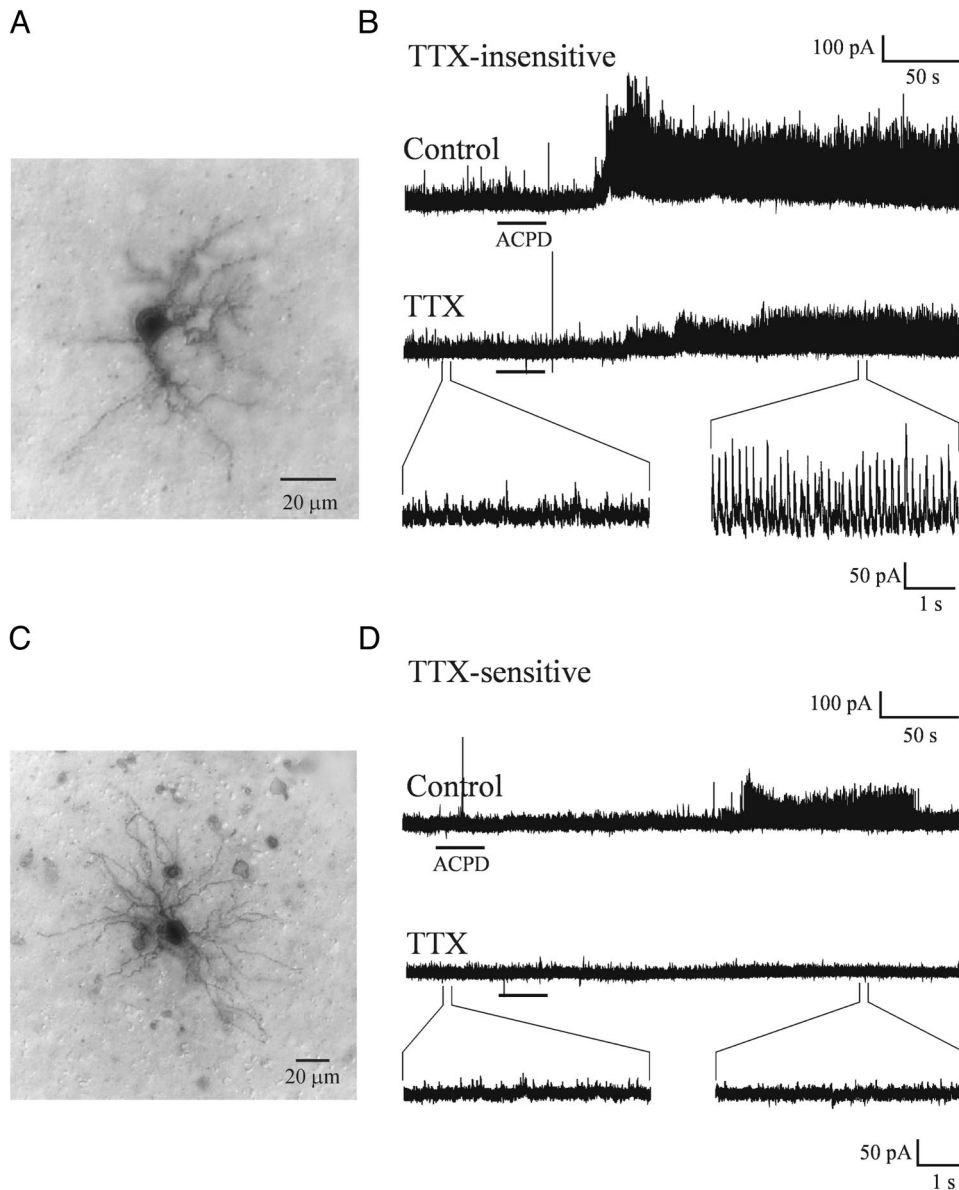


FIG. 8. Photomicrographs and responses of an “X-like” and a “Y-like” rat geniculate cell. *A*: an X-like cell, characterized by a small number of primary dendrites and a more bipolar dendritic arbor. *B*: recordings from the cell shown in *A*. *Top*: the increase in sIPSC activity in response to ACPD. *Middle*: the response to ACPD persists in the presence of TTX (1 μ M). *Bottom 2 traces*: the responses at a faster time scale, individual sIPSCs at a larger time scale. *C*: Y-like cell with more primary dendrites and radially symmetrical dendritic arbors. *D*: recordings of the cell in *C*. The response to ACPD (*top*) was abolished completely by the application of TTX (1 μ M; *middle*). The blockade of the response to ACPD can be seen more clearly at larger time scale (*bottom*).

class. The finding that TTX insensitivity seems to vary widely among cells does not necessarily mean that there is an equivalent variability among cells in the morphological extent of triadic circuitry because we cannot assume a monotonic relationship between numbers of triads and extent of the TTX-insensitive response. Many other variable factors can be involved, including baseline sIPSC activity, state of the interneurons giving rise to the dendritic terminals involved in triads, alterations made in the dendritic tree from brain slicing, etc. Nonetheless, it is somewhat surprising that the parameter of TTX sensitivity was unimodally distributed among geniculate cells in the cat, and some of the abovementioned issues could contribute to this. It is also possible that our use of juvenile animals, required for good whole cell recording, is another contributing factor and that had the experiments been done on fully adult animals a bimodal distribution would have been seen. This, however, is consistent with earlier data that, while X cells have more triadic circuitry than do Y cells, the difference is relative rather than absolute (Datskovskaia et

al. 2001; Friedlander et al. 1981; Hamos et al. 1987; Wilson et al. 1984).

Observations in the rat

With the exception of dendritic appendages, geniculate cells in the rat showed precisely the same correlations between morphology and TTX insensitivity as did those in the cat, suggesting a fundamental property of geniculate cells across species. Because triads are a ubiquitous feature of thalamus (reviewed in Sherman and Guillery 1996, 2002), this may also prove to be a general feature of thalamic relay cells.

However, despite the preceding correlations in the rat, the parameters measured were unimodally distributed, which fails to support the presence of more than a single class of geniculate relay cell. Of course, lack of evidence for separate geniculate cell classes in the rat does not constitute proof of one class. For example, our results can easily accommodate the possibility of two classes of rat relay cells with different but

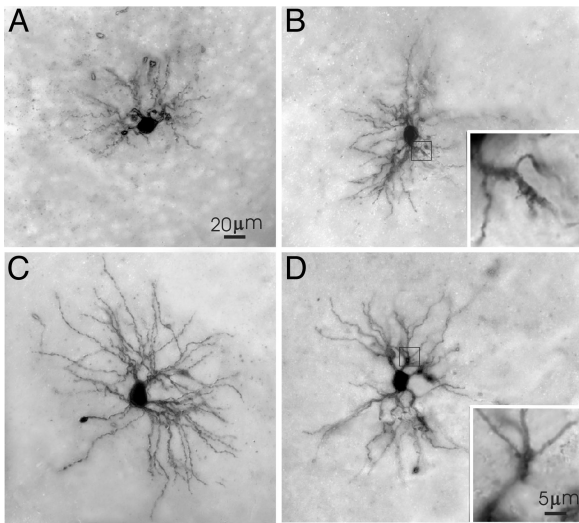


FIG. 9. More morphological examples of rat geniculate neurons. *A* and *B*: cells showing TTX-insensitive responses. *C* and *D*: cells showing TTX-sensitive responses. *Insets*: the appendages at primary branch points at higher magnification.

overlapping morphological and physiological variables measured in this study.

Of particular interest is the one striking difference between rat and cat: the correlation of TTX sensitivity with dendritic appendages at proximal branch points. In the case of the cat, it has been established that these appendages do represent the postsynaptic location of triadic inputs (Wilson et al. 1984;

Hamos et al. 1987). However, no such relationship has yet been documented for the rat. The possibility is thus raised here that these appendages do not necessarily imply triadic inputs and are thus not a universally interpreted feature of mammalian thalamus.

General conclusions

Triadic circuitry involving primary inputs to thalamic relays identified as “drivers” (Sherman and Guillery 1998), dendritic outputs of interneurons, and relay cells is ubiquitous to thalamus. The data reported here suggest that such circuitry is distributed among relay cells nonrandomly in the sense that it is correlated with a number of morphological parameters. More evidence is needed to determine how widespread these relationships are and whether they tend to form bimodal or continuously varying distributions.

CELLS IN THE CAT. Perhaps the best known classification of thalamic relay cells is the division of geniculate cells in the cat into X and Y classes. However, this has been based primarily on receptive field criteria (reviewed in Sherman 1985), and this, in turn, is a reflection of properties already present in their X or Y retinal afferents. Thus it was not clear in the original classification of these geniculate cells the extent to which there was any further difference between classes other than retinal input. Friedlander et al. (1981) established by intracellular labeling that there were clear anatomical differences, suggesting further elaboration of these classes, but these anatomical studies never established whether morphological differences

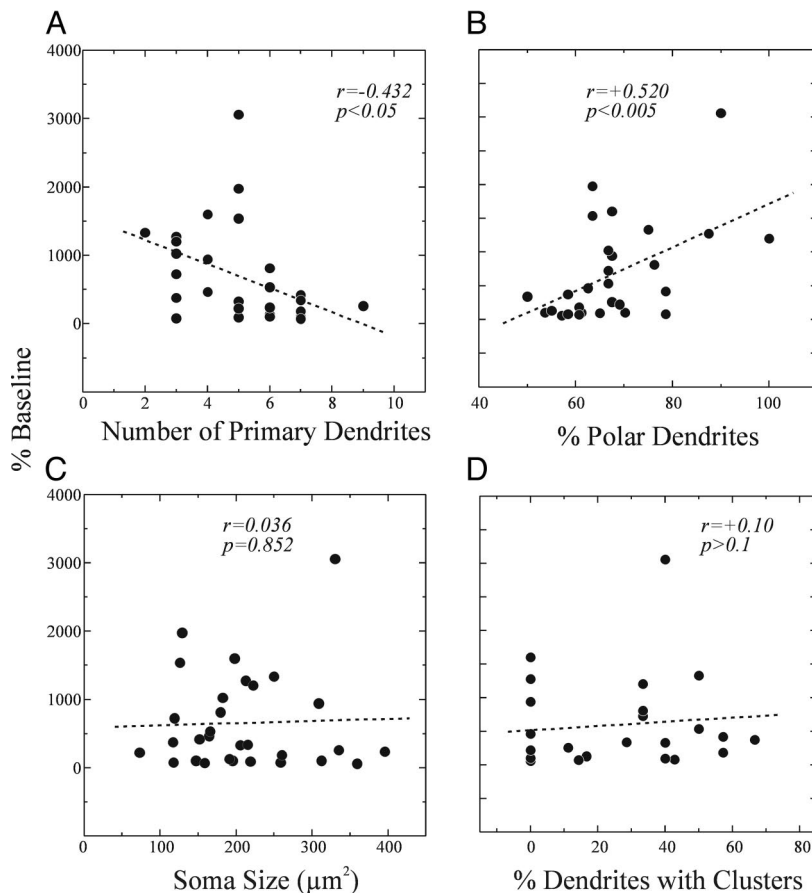


FIG. 10. Scatterplots showing measurements of morphological features of rat geniculate neurons and their relationships to the size of TTX-independent ACPD-evoked response measured as the percentage of the power between 3 and 30 Hz over the baseline; conventions as in Fig. 5. The number of cells is 30 for *A–C* and 25 for *D*. *A*: number of primary dendrites. This is significantly correlated with the size of the TTX-independent response. *B*: percentage of polar primary dendrites. This is also significantly correlated with the size of the TTX-independent response. *C*: cross-sectional area of the soma. This is not significantly correlated with the size of the TTX-independent response. *D*: percentage of primary branch points with grape-like appendages. This is not significantly correlated with the size of the TTX-independent response.

were bimodally distributed. Later studies with the electron microscope indicated that retinal input to X cells were nearly always triadic in nature, whereas those to Y cells were not (Hamos et al. 1987; Wilson et al. 1984), although the extent of this difference was recently called into question (Datskovskaia et al. 2001). The present results in the cat are consistent with the earlier study of Friedlander et al. (1981) and further suggest that the one truly distinctive difference between classes at the thalamic level in the cat may be the presence of dendritic appendages clustered at primary branch points.

CELLS IN THE RAT. The results in the rat from the present study are in most ways quite similar to those in the cat, suggesting clear morphological correlates with the presence of triadic innervation. Nonetheless, the curious lack of any correlation between the presence of dendritic appendages and triadic input raises doubts about the generality of this relationship for other thalamic nuclei where triadic relationships are found. This requires further study.

What is missing for the lateral geniculate nucleus of the rat is any clear neuronal classification based on receptive field properties analogous to the X/Y division that might be linked to the findings reported here. Attempts to date to classify rat geniculate cells have failed to do so conclusively (Fukuda et al. 1975 1979; Hale and Sefton 1978; Martin 1986; Reese 1988; Gabriel et al. 1996). This leaves two possibilities, among others: relationships between triadic input and certain morphological variables of relay cell exist, but these do not routinely correlate to different types of driver input as they do in the cat's lateral geniculate nucleus, or such a correlation does indeed exist, and the proper classification of retinogeniculate remains to be done for the rat.

ACKNOWLEDGMENTS

We thank S. Van Horn for expert technical assistance.

Present addresses: C. L. Cox, Dept. of Molecular and Integrative Physiology, University of Illinois, 524 Burrill Hall, 407 S. Goodwin Ave., Urbana IL 61801; Y.-W. Lam, C. Varela, and S. Murray Sherman, Dept. of Neurobiology, Pharmacology, and Physiology, The University of Chicago, 947 E. 58th St., Chicago, IL 60637.

GRANTS

This research was supported by National Eye Institute Grant EY-03038 and the Fundación Pedro Barrié de la Maza.

REFERENCES

- Cox CL and Sherman SM.** Control of dendritic outputs of inhibitory interneurons in the lateral geniculate nucleus. *Neuron* 27: 597–610, 2000.
- Datskovskaia A, Carden WB, and Bickford ME.** Y retinal terminals contact interneurons in the cat dorsal lateral geniculate nucleus. *J Comp Neurol* 430: 85–100, 2001.
- Fotuhi M, Sharp AH, Glatt CE, Hwang PM, Von Krosigk M, Snyder SH, and Dawson TM.** Differential localization of phosphoinositide-linked metabotropic glutamate receptor (mGluR1) and the inositol 1,4,5-trisphosphate receptor in rat brain. *J Neurosci* 13: 2001–2012, 1993.
- Friedlander MJ, Lin C-S, Stanford LR, and Sherman SM.** Morphology of functionally identified neurons in lateral geniculate nucleus of the cat. *J Neurophysiol* 46: 80–129, 1981.
- Fukuda Y, Sugitani M, and Kim Y.** A further study on fast and slow principal cells of rat lateral geniculate body: an analysis of flash-evoked responses. *Tohoku J Exp Med* 115: 33–45, 1975.
- Fukuda Y, Sumitomo I, Sugitani M, and Iwama K.** Receptive-field properties of cells in the dorsal part of the albino rat's lateral geniculate nucleus. *Jpn J Physiol* 29: 283–307, 1979.
- Gabriel S, Gabriel HJ, Grützmann R, Berlin K, and Davidowa H.** Effects of cholecystokinin on Y, X, and W cells in the dorsal lateral geniculate nucleus of rats. *Exp Brain Res* 109: 43–55, 1996.
- Godwin DW, Van Horn SC, Eri ir A, Sesma M, Romano C, and Sherman SM.** Ultrastructural localization suggests that retinal and cortical inputs access different metabotropic glutamate receptors in the lateral geniculate nucleus. *J Neurosci* 16: 8181–8192, 1996.
- Govindaiah and Cox CL.** Synaptic activation of metabotropic glutamate receptors regulates dendritic outputs of thalamic interneurons. *Neuron* 41: 611–623, 2004.
- Hale PT and Sefton J.** A comparison of the visual and electrical response properties of cells in the dorsal and ventral lateral geniculate nuclei. *Brain Res* 153: 591–595, 1978.
- Hamos JE, Van Horn SC, Raczkowski D, and Sherman SM.** Synaptic circuits involving an individual retinogeniculate axon in the cat. *J Comp Neurol* 259: 165–192, 1987.
- Lennie P and Perry VH.** Spatial contrast sensitivity of cells in the lateral geniculate nucleus of the rat. *J Physiol* 315: 69–79, 1981.
- Lieberman AR.** Neurons with presynaptic perikarya and presynaptic dendrites in the rat lateral geniculate nucleus. *Brain Res* 59: 35–59, 1973.
- Martin PR.** The projection of different retinal ganglion cell classes to the dorsal lateral geniculate nucleus in the hooded rat. *Exp Brain Res* 62: 77–88, 1986.
- Ohara PT, Lieberman AR, Hunt SP, and Wu JY.** Neural elements containing glutamic acid decarboxylase (GAD) in the dorsal lateral geniculate nucleus of the rat; immunohistochemical studies by light and electron microscopy. *Neurosci* 8: 189–211, 1983.
- Okamoto N, Hori S, Akazawa C, Hayashi Y, Shigemoto R, Mizuno N, and Nakanishi S.** Molecular characterization of a new metabotropic glutamate receptor mGluR7 coupled to inhibitory cyclic AMP signal transduction. *J Biol Chem* 269: 1231–1236, 1994.
- Reese BE.** “Hidden lamination” in the dorsal lateral geniculate nucleus: the functional organization of this thalamic region in the rat. *Brain Res Rev* 13: 119–137, 1988.
- Romano C, Sesma MA, McDonald CT, O'Malley K, Van den Pol AN, and Olney JW.** Distribution of metabotropic glutamate receptor mGluR5 immunoreactivity in rat brain. *J Comp Neurol* 355: 455–469, 1995.
- Sherman SM.** Functional organization of the W-, X-, and Y-cell pathways in the cat: a review and hypothesis. In: *Progress in Psychobiology and Physiological Psychology*, edited by Sprague JM and Epstein AN. Orlando, FL: Academic, 1985, vol. 11, p. 233–314.
- Sherman SM and Guillery RW.** The functional organization of thalamocortical relays. *J Neurophysiol* 76: 1367–1395, 1996.
- Sherman SM and Guillery RW.** On the actions that one nerve cell can have on another: distinguishing “drivers” from “modulators.” *Proc Natl Acad Sci USA* 95: 7121–7126, 1998.
- Sherman SM and Guillery RW.** The role of thalamus in the flow of information to cortex. *Philos Trans R Soc Lond [Biol]* 357: 1695–1708, 2002.
- Sherman SM and Guillery RW.** Thalamus. In: *Synaptic Organization of the Brain*, edited by Shepherd GM. Oxford, UK: Oxford Univ. Press, 2004a, p. 311–359.
- Sherman SM and Guillery RW.** The visual relays in the thalamus. In: *The Visual Neurosciences*, edited by Chalupa LM and Werner JS. Cambridge, MA: MIT Press, 2004b, p. 565–591.
- Shigemoto R, Nakanishi S, and Mizuno N.** Distribution of the mRNA for a metabotropic glutamate receptor (mGluR1) in the central nervous system: an in situ hybridization study in adult and developing rat. *J Comp Neurol* 322: 121–135, 1992.
- Stanford LR, Friedlander MJ, and Sherman SM.** Morphological and physiological properties of geniculate W-cells of the cat: a comparison with X- and Y-cells. *J Neurophysiol* 50: 582–608, 1983.
- Tanabe Y, Normura A, Masu M, Shigemoto R, Mizuno N, and Nakanishi S.** Signal transduction, pharmacological properties, and expression patterns of two rat metabotropic glutamate receptors, mGluR3 and mGluR4. *J Neurosci* 13: 1372–1378, 1993.
- Wilson JR, Friedlander MJ, and Sherman SM.** Fine structural morphology of identified X- and Y-cells in the cat's lateral geniculate nucleus. *Proc Roy Soc Lond B* 221: 411–436, 1984.